

# We are IntechOpen, the world's leading publisher of Open Access books Built by scientists, for scientists

6,900

Open access books available

186,000

International authors and editors

200M

Downloads

Our authors are among the

154

Countries delivered to

TOP 1%

most cited scientists

12.2%

Contributors from top 500 universities



WEB OF SCIENCE™

Selection of our books indexed in the Book Citation Index  
in Web of Science™ Core Collection (BKCI)

Interested in publishing with us?  
Contact [book.department@intechopen.com](mailto:book.department@intechopen.com)

Numbers displayed above are based on latest data collected.  
For more information visit [www.intechopen.com](http://www.intechopen.com)



# Determination of Essential Parameters for Quality Control in Fabrication of Piezoelectric Micropumps

*Matej Možek, Borut Pečar, Drago Resnik and Danilo Vrtačnik*

## Abstract

Quality control of piezoelectric micropumps is presented through design, fabrication process, operation, and characterization. The presented study resulted in the extraction of a minimal set of monitored parameters, which is a prerequisite for reliable and stable micropump operation. Micropump fabrication process steps, especially bonding process quality, in correlation with quality control of micropump constituent components (housing, elastomer, and piezoelectric actuator) provided an explanation for deterioration of common micropump characteristics, such as flow vs. backpressure, suction pressure, and excitation signal. These characteristics also manifested in deterioration of other important micropump properties, such as self-priming ability, bubble tolerance, long-term stability, heat dissipation, and temperature operating range. Besides air and DI water pumping, chemical compatibility of constituent materials was confirmed during successful long-term testing of micropumps by pumping media with different viscosity and aggressive media with low pH value. The extracted set of parameters defines input control for micropump fabrication process while at the same time establishes safe operating area of fabricated micropumps. The presented set of parameters provides quality control guidelines and enables a direct comparison from pump-to-pump or run-to-run variations and extraction of influencing design or fabrication parameters.

**Keywords:** microcylinder pump, self-priming, bubble tolerance, PZT actuator

## 1. Introduction

Micropumps are essential components of microfluidic systems. Due to their small size, energy efficiency, low fabrication cost, high performance, and reliability, they are extensively versatile in vital areas of human activities. Application fields for micropumps span from microprocess engineering, medical applications, and diagnostics, to cooling the electronic devices, microtool lubrication, and beyond. Among those activities, an important segment of use includes controlled flow management of the reagents in microfluidic chips for biomedical applications [1], chemical process engineering [2], biochemistry [3], and pharmacy [4], where they can be employed in the system separately or in an integrated form. In order to fully

understand the micropump behavior in various applications, micropump as a whole and its constituent parts (piezoelectric disk, elastomer, interlayer adhesive, and plastic housing) have to be thoroughly characterized by taking into account a wide range of parameters. Deterioration of inherent micropump characteristics, such as flow vs. backpressure, suction pressure, and excitation signal are manifested in deterioration of other important properties of micropumps, such as self-priming ability, bubble tolerance, long-term stability, and temperature operating range. Additionally, the quality of micropump system performance is affected by other factors such as viscosity and pH of pumping media, as well as waveform, amplitude, and frequency of excitation signal. All these factors can be explained by the analysis of physical parameter measurements related to evaluation of individual micropump components. Correlations between abovementioned deterioration origins result in a minimal set of dominant monitored parameters, prerequisite for reliable and stable micropump operation. Extracted parameters define input control for micropump fabrication process, while at the same time establishing safe operating area of fabricated micropumps.

The chapter will briefly present micropump design and operation, followed by the description of above-listed micropump characterization methods, which enable quality control. Beside the typical flow rate and backpressure characteristics of the micropump, influence of properties, such as self-priming, bubble tolerance, pumping media compatibility, long-term stability, and temperature dependencies, has been under investigation, and their impact on overall micropump performances has been evaluated. Characterization methods and protocols were established for each of the abovementioned micropump parameters under investigation. Among them, the most relevant characterized parameters for reliable micropump operation will be defined, and correlations which are leading back to constituting components and correlations among them will be presented. Microsystem interactions through pumping media and excitation signal will be thoroughly analyzed, and a resulting set of input parameters in the fabrication of piezoelectric micropumps will be determined. This set of parameters provides quality control guidelines and enables a direct comparison from pump-to-pump or run-to-run variations and extraction of influencing design or fabrication parameters.

## **2. Case study: microcylinder pump**

An innovative microcylinder pump, developed in our laboratory, was selected for a case study of micropump quality control. Microcylinder pump design does not employ any check valves. Instead, it operates on a principle of active sequential expansion (opening) and compression (closing) of the centrally placed inlet cylindrical rectifying element and outlet throttle rectifying element. The expansion/compression is performed by an actuated glass membrane that is loosely attached via a resilient elastomer to the top of the supporting glass. Exploded view of a typical thermoplastic (TP) microcylinder pump structure with constituent materials and corresponding bonding processes is shown in **Figure 1**.

The TP microcylinder pump comprises polydimethylsiloxane (PDMS) elastomer layer with molded micropump chamber, fluidic microchannel, and rectifying elements (**Figure 1c**). Additionally, two through-holes are punched into an elastomer, one into the center of the micropump chamber and the other one at the end of the channel. PDMS elastomer layer (**Figure 1c**) and PDMS fluidic connections (**Figure 1e**) are covalently bonded to the supporting TP substrate (**Figure 1d**) by employing developed amine-PDMS linker bonding process. One inlet and one outlet fluid port is drilled through a supporting TP substrate that supply and drain the

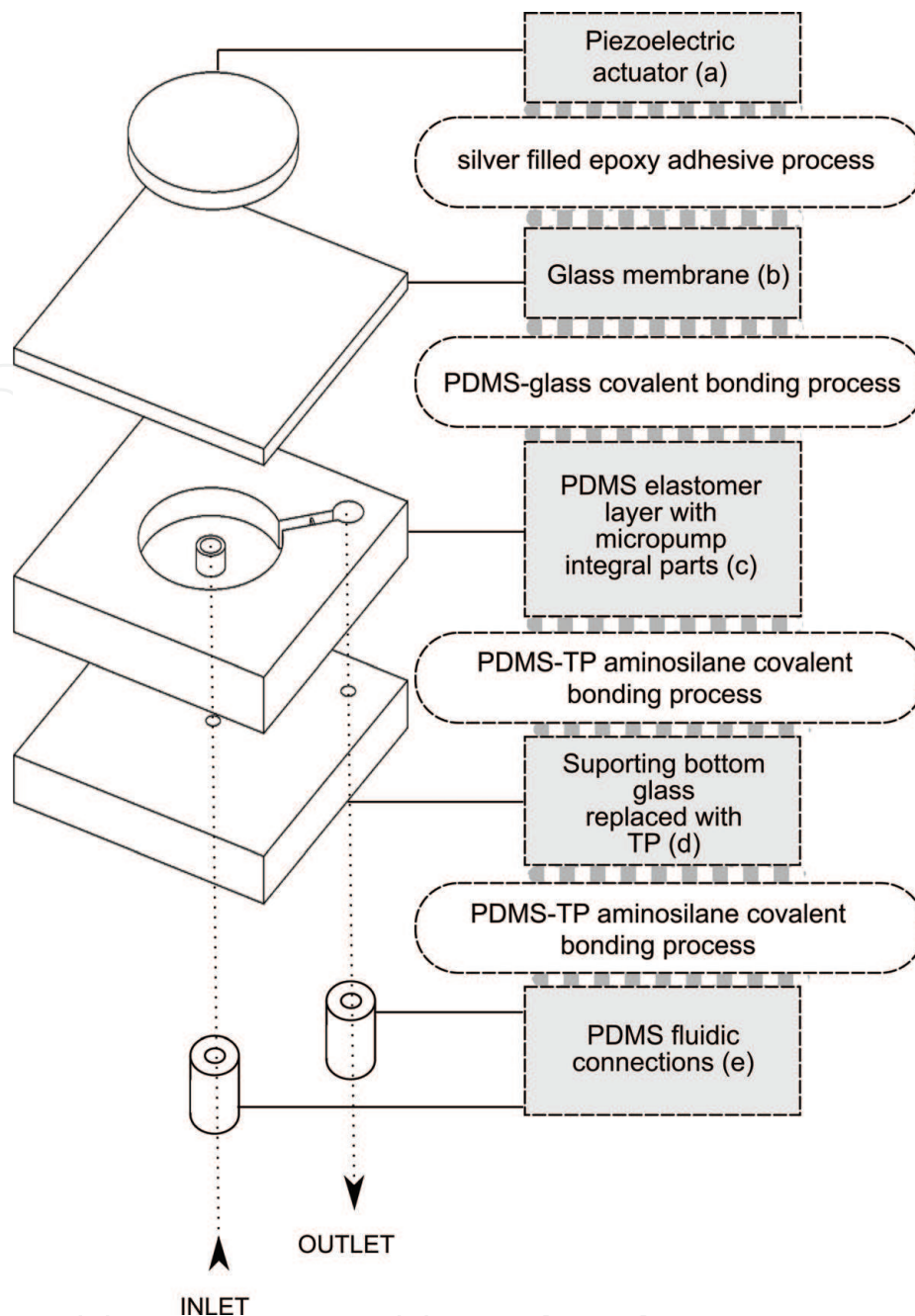


**Figure 1.** Exploded view of a typical TP microcylinder pump structure with constituent materials (a - Piezoelectric actuator, b - thin glass membrane, c - PDMS elastomer layer with micropump chamber, fluidic microchannel, and rectifying elements, d - supporting TP substrate, e - PDMS fluidic connections) and corresponding bonding processes (dimensions are not to scale).

fluid into and out of the pump. The micropump chamber and the microchannel are sealed with a thin glass membrane (**Figure 1b**) by employing oxygen plasma PDMS-glass covalent bonding process. Piezoelectric actuator (**Figure 1a**) is positioned in the axis of a micropump chamber, coupled rigidly to the micropump membrane through silver-filled epoxy adhesive (EPO-TEK EE129-4, Billerica, MA, USA).

Microcylinder pump operation is depicted in **Figure 2**, which is showing (a) the micropump with no excitation signal applied and two distinctive operation cycle phases, (b) pumping phase and (c) suction phase. During excitation, loosely attached glass membrane and PDMS elastomer layer deform in a controlled manner, which enables compression and expansion of the centrally placed inlet cylindrical port, micropump chamber, and outlet throttle shaped port with a specific phase lag, contributing to efficient micropump operation.

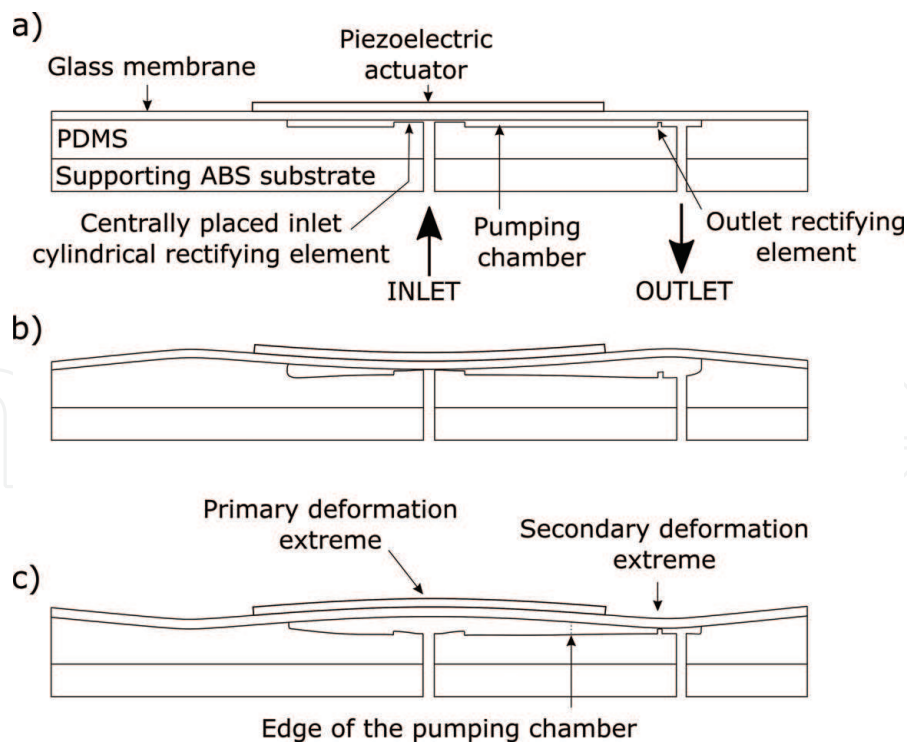


**Figure 2.** Microcylinder pump operation cycle: (a) No excitation signal applied, (b) suction phase (membrane expansion), and (c) pumping phase (membrane compression).

Detailed microcylinder operation and fabrication process is reported elsewhere [5].

### 3. Fabrication quality control

#### 3.1 Quality control of micropump housing

Micropumps were first developed on flat ABS substrates. In this case, surface flatness of ABS is usually in the range 5–7  $\mu\text{m}$  and does not introduce any notable stress in glass membrane after covalent bonding, which would result in micropump performance deterioration. In a more mature phase of development, efforts were focused toward industrial product. Therefore, ABS housing was developed with corresponding changes to adapt all the previous assembly steps. The influence of specific housing construction and adapted process steps should be therefore carefully evaluated in terms of micropump performances. The flatness of the injection molded ABS housing, which serves as a micropump substrate, was found to be critical, since the PDMS and glass membrane are attached by covalent bonding directly on flat part of ABS housing. Irregular flatness of ABS substrate directly transfers on the membrane via strong chemical bonds and results in a local mechanical stress.

Quality of the surface relief should be closely monitored in the stage of injection molding by adjusting the process parameters. Prior to optimization, the surface topography scans (**Figure 3a**) showed flatness tolerance around 40  $\mu\text{m}$  with high gradients that resulted in poor yield and low flowrate and backpressure performances. The stress in glass membrane can further affect the pump behavior via severely decreasing the throttle valve gap, consequently causing spontaneous sticking of PDMS and glass and ultimately a malfunction.

After adjusting the injection molding process parameters, we were able to achieve flatness comparable with flat substrates and were below 10  $\mu\text{m}$  across  $2 \times 2 \text{ cm}^2$  area of the housing size, which is shown in **Figure 3b**.

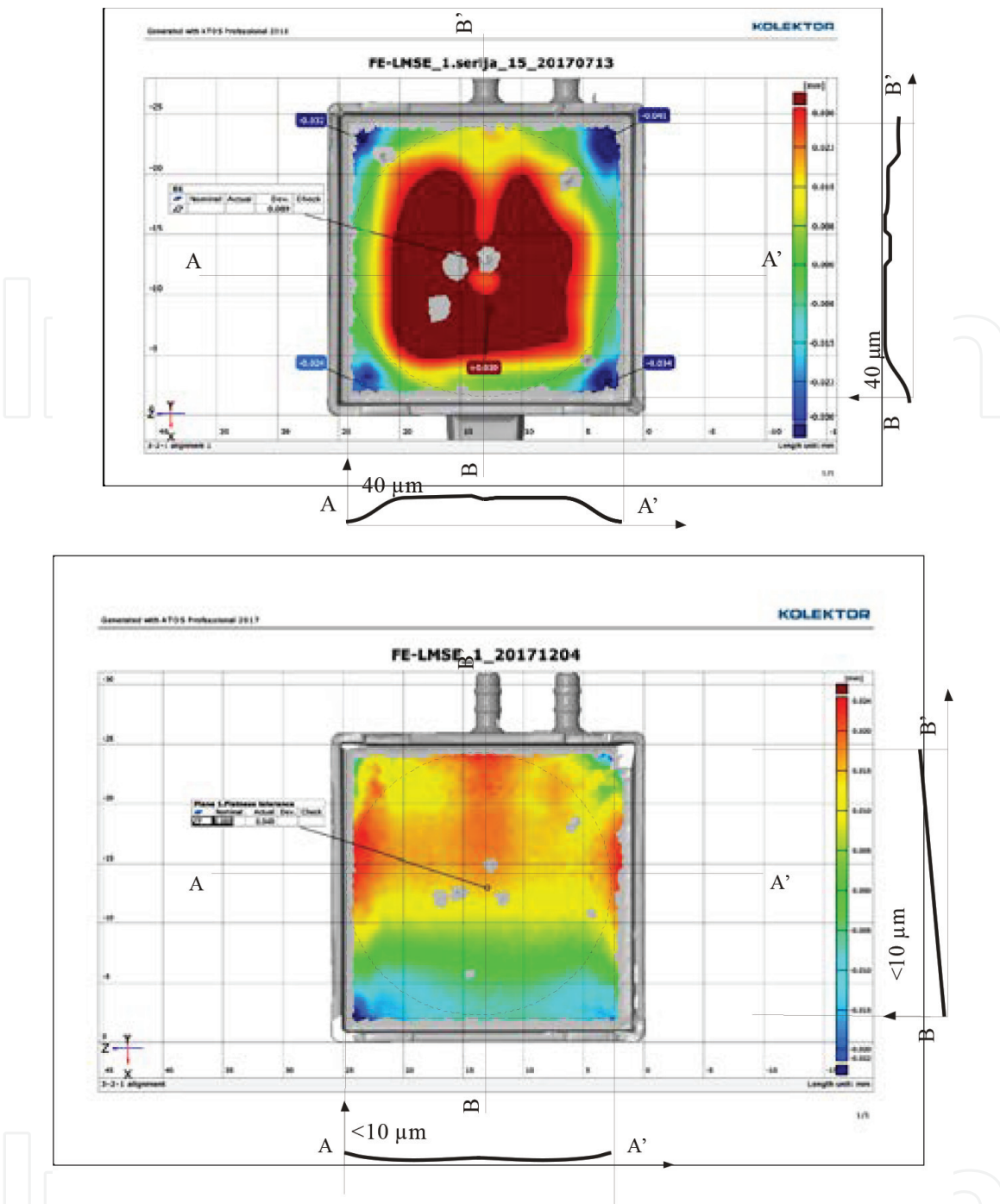


**Figure 3.** Flatness profiles of (a) irregular surface in the early stage of development causing frequent micropump malfunction and (b) surface that fulfills the tolerance range of micropump performances and reliable operation (Kolektor Group, Idrija, Slovenia).

Flatness tolerance below 10 µm was found to accommodate bonded layers, keeping them in low-stress regime, thus, without affecting the pump performance. This measurement with established tolerance was found to be one of the prerequisites in a sequence of quality control steps.

### 3.2 Quality control of micropump bonding process

Covalent bonding of constituent micropump components during fabrication process has many advantages over use of adhesives. Covalent bonding does not introduce any additional materials, which would get in contact with aggressive pumping media. Due to absence of glue, micropump fluidic structures cannot be contaminated or even clogged during fabrication process.

Many strategies for plastic-PDMS bonding have been reported, such as sol-gel coating approach, chemical gluing approach, and organofunctional silanes approach [6, 7], where thermoplastics in the presence of amine undergo aminolysis followed by chain scission of the carbonyl backbone, forming a strong urethane bond. One of organofunctional silanes is amine-PDMS linker (poly [dimethyl siloxane-co-(3-aminopropyl) methyl siloxane]). Amine-PDMS linker incorporates an amine functionality at one terminal and a segment of low-molecular-weight PDMS at the other, which provide better hydrolytic bond stability over commonly employed organofunctional silane APTES [8].

In our micropump fabrication process, thermoplastic (TP) substrates are cleaned in ultrasonic bath, followed by silylation of the surfaces through the use of amine-PDMS linker. After plasma activation, the activated surfaces of the two substrates are brought into contact, using methanol as an aligning medium. Detailed bonding process procedure was reported elsewhere [9].

It is reasonable to evaluate bond strength by employing effective destructive methods on simple burst pressure test devices rather than on fabricated micropumps. Pressure regulated air supply is connected to the inlet of the test device and the pressure at which the device fails is determined. Burst pressure test devices enable optical observation of bond failure at fluidic channel sharp corners, where the structural stress caused by applied fluidic pressure is the largest. Burst pressure tests should be performed with water and compressed air.

Our burst pressure tests confirmed hydrolytic stability of TP-PDMS bonds established through amine-PDMS linker [9]. It is speculated that the water-repelling nature of the PDMS component in amine-PDMS linker prevents penetration of the aqueous solutions at the interface improving bond hydrolytic resistance [10, 11].

### 3.3 Elastomer mechanical properties control

Mechanical properties of viscoelastic PDMS material, which is one of the crucial parts of here discussed micropump, are mainly influenced by mixing ratio, curing temperature process, and additional aging at moderate temperatures to stabilize the polymer. It is therefore mandatory to determine the appropriate parameters in the preparation phase that can later affect the micropump operation.

According to our measurements and evaluations performed, micropump flow rate and backpressure performance depend strongly on curing temperature of PDMS polymer as shown in **Figure 4**.

In this particular experiment, four microcylinder pumps were fabricated differing only in PDMS elastomer curing temperature setting during fabrication process. First sample underwent our standard curing temperature of 80°C, and three others underwent curing temperatures of 110, 150, and 200°C. Curing time at all selected curing temperatures was set to 2 hours. After the micropumps were assembled, they were additionally exposed to a setting temperature of 80°C for 14 hours. This process step is a standard step in our well-established micropump fabrication process and was initially introduced in order to stabilize covalent bonds between constituent materials.

It was shown that DI flow rate can be reduced by more than 50%, if curing temperature is increased from 80 to 200°C. Correspondingly, Young modulus of elasticity ( $E$ ) from the literature [12] increases by 61% in this temperature range. Increased PDMS curing temperature reflects in greater stiffness of elastomer layer, which impairs the magnitude of membrane deformation, pumping stroke volume, and rectifying elements efficiency. By taking into account the same base to

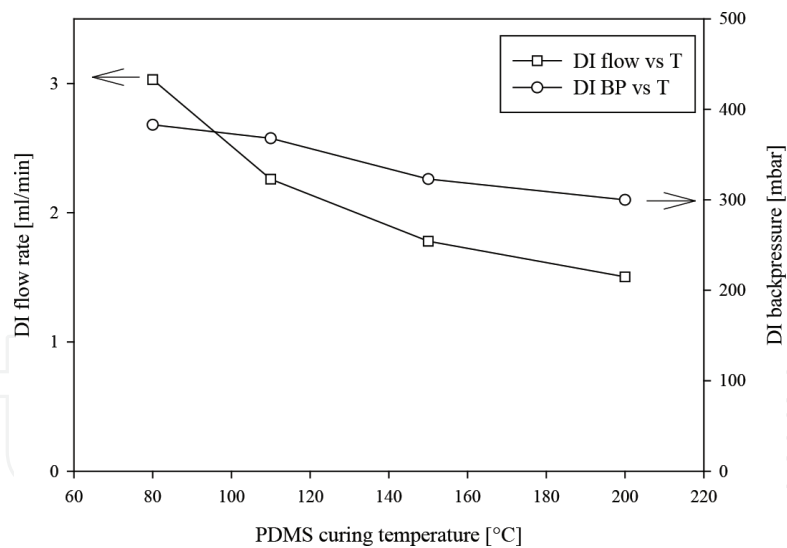


**Figure 4.**  
*Micropump flow rate and backpressure performance vs. curing temperature of PDMS polymer.*

polymerization component ratio, increased Young modulus of elasticity is in agreement with reduced DI flow rate.

#### 4. Essential micropump measurements for quality control

An automated system for micropump characterization was designed. Such system comprises a high voltage waveform generator, which is connected to a PC and a dedicated computer software that automatically drives the micropumps and simultaneously saves measured flowrate or back pressure data. Instantaneous water flowrate can be measured with flow meter or as in our case computed by gravimetric method ( $Q = dm/dt \rho$ ), employing a precision scale connected to a PC. If gravimetric method is used, the water level of collecting tank on the scale should be matched with water level of storage tank by placing the tank on laboratory elevator. To minimize evaporation of water from a surface of an open collecting tank, the tank can be shaped as a cylinder with a small diameter. Falling droplets can be avoided by pre-filling the collection tank with tare amount of water.

In our case, excitation signal frequency at constant amplitude or vice versa is swept automatically (0–300 Hz with step of 5 Hz every 10 s and 0–250 V with step of 5 V every 10 s, respectively). Instantaneous air flowrate is measured with Microbridge Mass Airflow Sensor (AWM3150V, Honeywell, NJ, USA), while instantaneous backpressure/suction pressure of both water and air is measured with calibrated differential pressure sensor (HCX005D6V, First Sensor AG, Berlin, Germany). Both are connected to PC via digital multimeter Keithley 2700 (Keithley instruments, OH, USA).

First, frequency sweeps are performed up to 300 Hz at maximum admissible amplitude in order to determine optimal performance frequency for a given pumping medium. After the optimal frequency is evaluated, the amplitude sweeps are performed up to maximum admissible value at optimal excitation frequency. In both measuring procedures, flowrate or backpressure/suction pressure data are simultaneously acquired. An example of measured performance characteristics is shown in **Figure 5** [5].

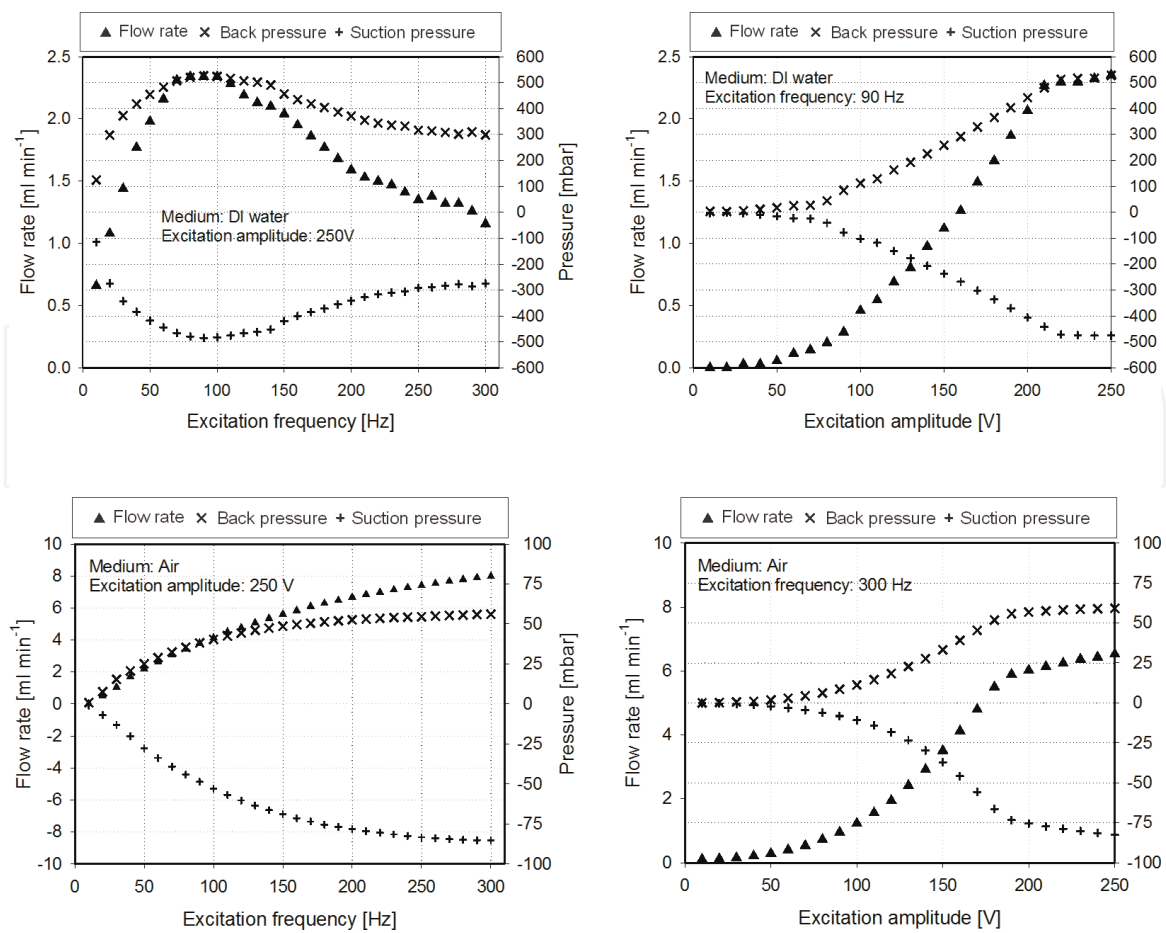


**Figure 5.** Flow rate, backpressure, and suction pressure vs. excitation signal frequency and excitation signal amplitude characteristics for DI water and air.

## 5. Additional parameters for assessing pump quality

### 5.1 Quality control of PZT actuator

PZT actuator converts one part of electrical energy into mechanical energy needed for micropump operation. Ferroelectric ceramics are subjected to degradation either during electrical loading (fatigue) or with time in the absence of an external mechanical or electrical load (aging) [13].

To assess the stability of piezoelectric actuator, piezoelectric  $d_{33}$  modulus measurements were performed first on unattached piezoelectric actuators using  $d_{33}$  piezometer PM10 (@100 Hz). Measuring of  $d_{33}$  modulus is fast and easy to perform in opposition with  $d_{31}$  modulus that requires advanced and time-consuming measuring methods. It was assumed that measured  $d_{33}$  modulus and essential  $d_{31}$  modulus that affect micropump operation are proportional to each other. Degradation of  $d_{31}$  modulus is our core concern as it directly affects micropump flowrate and backpressure performance stability.

Piezometer  $d_{33}$  system implements Berlincourt method. After clamping the sample and subjecting it to a low frequency force, the system processes the electrical signals from the sample, compares it with a built-in reference, and calculates  $d_{33}$  modulus. Modulus  $d_{33}$  implies an induced strain in direction of PZT disc rotation axis per unit electric field applied in the same direction.

First,  $d_{33}$  modulus stability over time was evaluated by applying stable square excitation waveform and custom generator waveform on unattached PZT samples

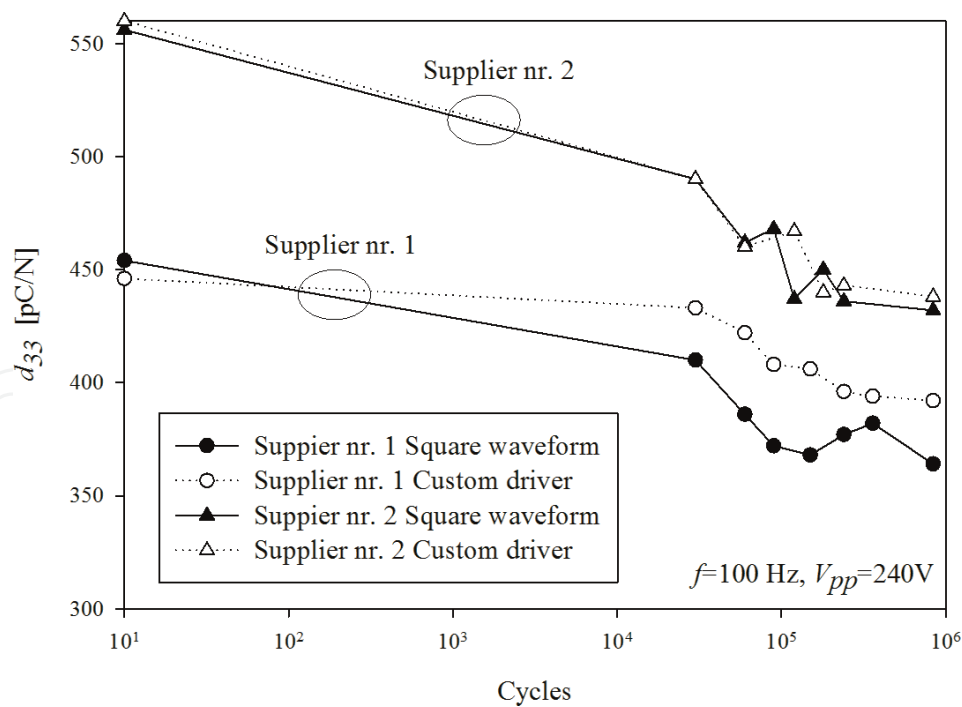


**Figure 6.**  
 PZT  $d_{33}$  modulus stability vs. switching cycles.

for 140 minutes in total. In between, the samples were repeatedly disconnected, clamped into  $d_{33}$  piezometer, measured, and then connected again to the driver. To minimize measurement error, samples were always clamped on the same central spot. **Figure 6** shows measured  $d_{33}$  modulus vs. number of switching cycles for two commercially available PZT samples for two applied waveforms with a frequency of 100 Hz and with an excitation amplitude of 120 V. For both PZT samples,  $d_{33}$  modulus decreased mainly in the first  $10^5$  switching cycles ( $-21\%$  for manufacturer nr. 1 and  $-19\%$  for manufacturer nr. 2), after that the downward trend was significantly reduced.

As expected,  $d_{33}$  modulus stability was affected also by excitation signal shape. In our case, square excitation waveform yielded greater decline ( $+9.3\%$  for manufacturer nr.1 sample and  $+6.3\%$  for manufacturer nr. 2 sample) in  $d_{33}$  modulus in first  $10^5$  switching cycles compared to custom driver waveform.

Next,  $d_{33}$  modulus stability was investigated regarding the amplitude of applied excitation signal. Before each  $d_{33}$  measurement, samples were driven with square excitation waveform for 10 seconds at preselected excitation signal amplitude values. Measurements on samples after initial operation by applying electric field yielded higher  $d_{33}$  values compared to measured off-the-shelf  $d_{33}$  values. It is also known from the literature that after poling step, the material microstructure tends to relax in logarithmical manner, thus decreasing the initial  $d_{33}$ .

After gradual incensement of excitation signal amplitude,  $d_{33}$  modulus decreased at a rate of  $-0.445$  pC/NV and  $-1.2$  pC/NV for manufacturer nr. 1 and nr. 2, respectively. Although manufacturer nr. 2 sample yielded higher initial  $d_{33}$  values compared to manufacturer nr. 1 sample, both performed equally at excitation signal amplitude of 160 V. However, manufacturer nr. 2 sample failed permanently at 180 V. Next,  $d_{33}$  modulus stability was investigated regarding the amplitude of applied excitation signal (**Figure 7**).

Regarding micropump operation, PZT fatigue effect is the most evident when measuring the dependency of flow rate vs. applied voltage on PZT. This is the property that deserves close attention when setting the safety margins (safe

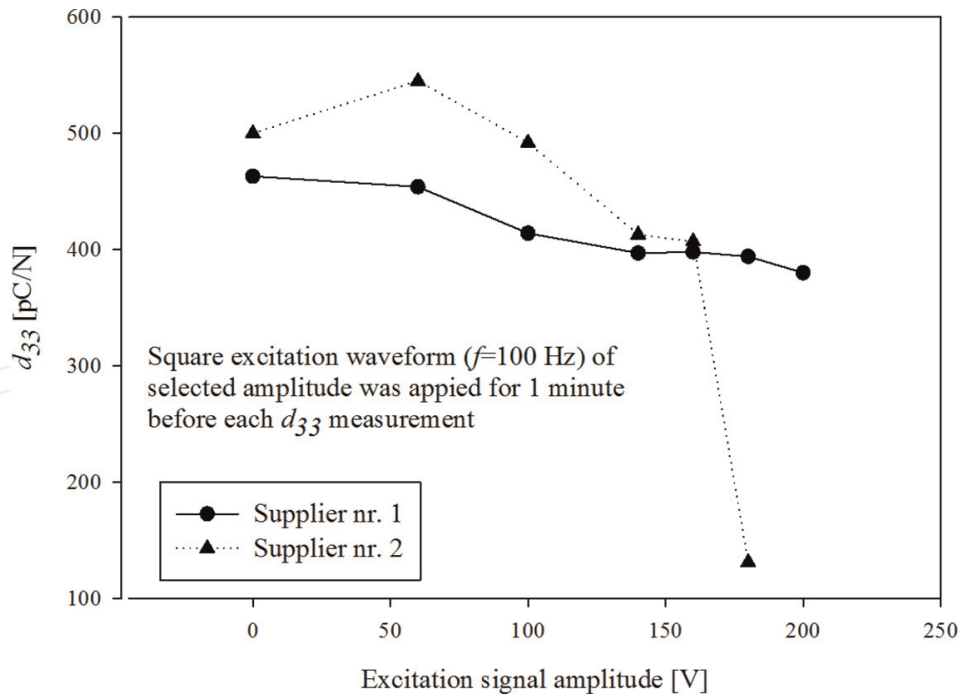


**Figure 7.**  
PZT  $d_{33}$  modulus stability vs. excitation signal amplitude.

operation area) and is one of quality criteria finally reflected through the pump performance deterioration.

**Figure 8** shows how flow rate increases linearly with excitation amplitude and is stable with time. This is true at each point shown until the amplitude level of 110 V for the presented case. However, when abovementioned amplitude was exceeded (which might be below the value specified by manufacturers), the flow does not respond in a linear manner and also the time stability of flow rate (as being checked at each point shown) is not maintained. After reverting to lower voltages again, the flow is irreversibly reduced, showing that PZT actuator is severely affected when

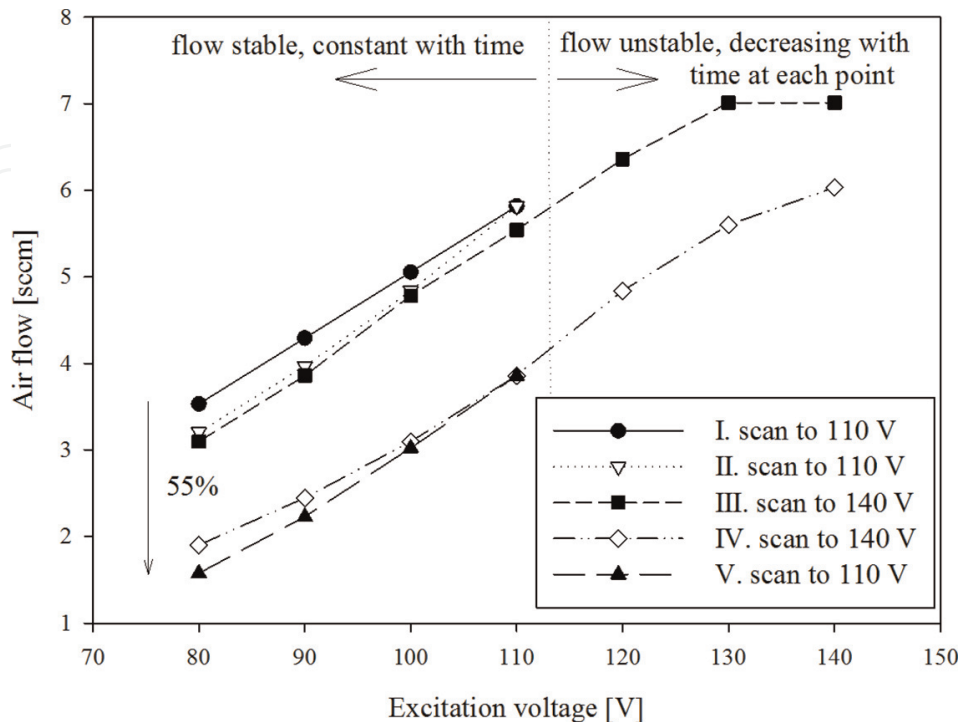


**Figure 8.**  
Excitation amplitude safe operation range and reduced flow when exceeding the limiting amplitude.

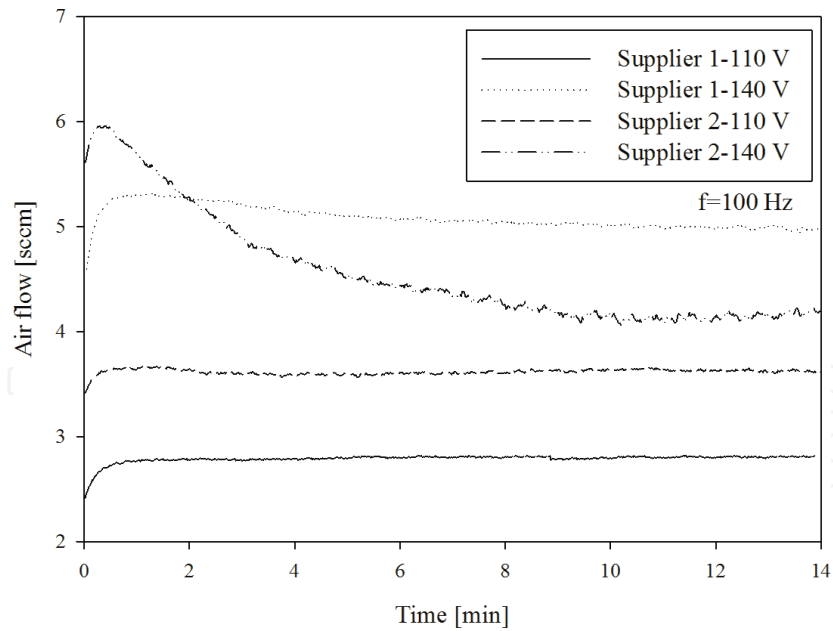


**Figure 9.**  
 Time stability for two types of PZT, driven at limiting amplitudes.

overdriven. Instead, it behaves as shown in **Figure 9**, and at 140 V, (shown for two distinct manufacturers) one preserved the air flow stability, the other deteriorated rapidly.

## 5.2 Micropump chemical compatibility

Constituent materials of the micropump being in direct contact with medium, each having its specific chemical and mechanical properties, should withstand long-term micropump operation without failure. It is therefore mandatory to determine their chemical resistance and fatigue issues. In this respect, a variety of media with distinct pH and different viscosities should also be included in micropump quality control test set. To provide reliable data in the specification list, the micropump tests were performed under continuous operation in the time period between 10 and 300 hours. A set of presented tests, summarized in **Table 1**, comprised common

Medium (/)	Dynamic viscosity (mPas)	pH (/)	Density (g/cm <sup>3</sup> )	Test time (hours)	Flow rate (ml/min)
DI water	1	6.5	1	24	1.73
City water	1	7.1	1	24	1.68
Glycol DG372	32	10	1.09	6	0.033
Saline 0.9% NaCl	1	7	1	6	1.62
PBS	1.07	7.4	1.06	6	1.61
Sn bath	NA	1	1.62	48	0.49
Ni bath	NA	4	1.64	90	0.37
1 M H <sub>2</sub> SO <sub>4</sub>	1.12	1	1.07	136	0.45
DI water after tests	1	6.5	1	1	1.71

**Table 1.**  
 Typical micropump performance evaluation for different media.

liquids that might be potentially encountered for pumping in a laboratory or industrial R&D environment.

Micropump materials exposed directly to the chemicals in the presented case are Tygon ND 100-65 tubes, ABS polymer substrate, glass membrane, and PDMS channel. Tests were performed by continuous pumping from a 5 ml reservoir of fluid in a closed loop system.

One criterion to reassure quality and compatibility was to monitor the flow rate variations over period of time. It can vary due to deterioration of materials themselves or due to particles that can cause obstructions in pumping chamber or in throttle region, since the tests were performed without any additional filtering. After the tests were completed, the flow rate of DI water should be maintained as compared to values obtained prior to tests. This will confirm that the constituent materials are chemically resistant to the media tested. Careful optical inspection of potential obstructions was found at throttle only due to unfiltered tap water and none of potential products (aggregates) due to unexpected chemical reaction between the aggressive media and pump materials. It should be kept in mind that for high viscosity medium, such as glycol, the excitation frequency should be lowered to obtain optimal flow rate. Phosphate-buffered solution (PBS) and physiological solution (0.9% NaCl) were also successfully pumped for 6 hours with constant flow rate, showing the pump is useful for biological experiments.

Furthermore, micropump was subdued to even more rigorous tests with a set of aggressive media to evaluate chemical resistance. One of the potential proposed applications of micropump was to periodically replenish small amounts of solutions in electroplating tin and nickel baths. Exact compositions of solutions given by industrial partner were not revealed, but are commonly used in metal electroplating industry. First, we determined pH and specific gravity of each to convert it into flow rate. It should be mentioned that during these tests, the same pump was used for all three liquids. DI water purging between each medium test was performed and exactly measuring a reference DI flow rate prior to, between the tests and after tests. Short term stability was first monitored for 2 hours for each media (**Figure 10**), followed by separate long-term tests (**Figure 11**). The properties of aggressive media, flow rate, and test duration are given in **Table 1**. The raw data can be further used to set the flow control loop.

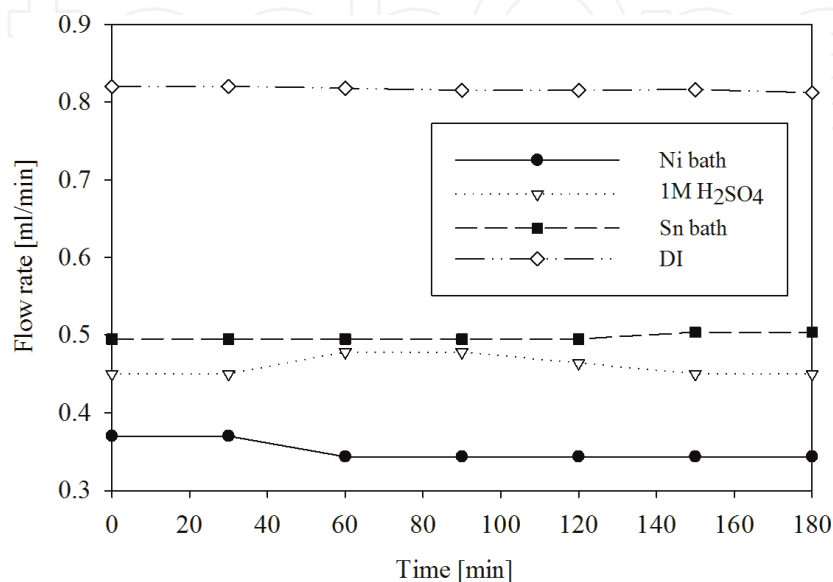


**Figure 10.** Continuous short-term pump operation for three aggressive media and DI water.

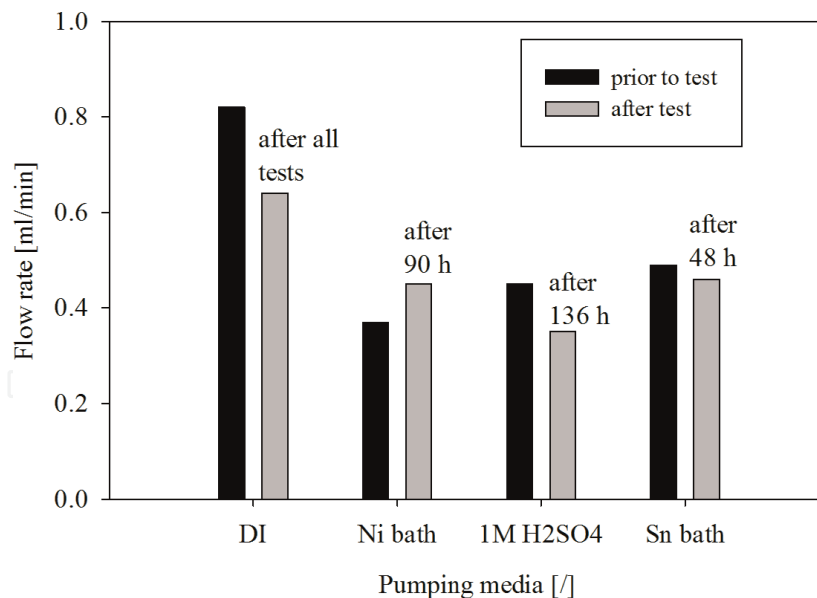


**Figure 11.**  
*Continuous long-term pump operation for three aggressive media and DI water.*

Alcohols and solvents are particular group of media that require careful consideration. PDMS, which is used in presented micropumps, is not compatible with latter as it is subdued to swelling when exposed to solvents. It was determined that swelling reduces the geometry of gaps and obstructs the flow irreversibly.

### 5.3 Self-priming

In principle, presented micropumps are intended to pump liquids, however, one of the figures of merit is the pump self-priming parameter, that is, the ability of the dry micropump to pump air until the liquid is dragged into the micropump chamber from the reservoir, which might be in certain cases located below the micropump level.

After several experimentally performed priming tests, it was determined that one should strictly distinguish between three approaches to define micropump priming property as the values may differ significantly: First approach is to measure air suction pressure (SP) at pump inlet by means of pressure sensor, with the outlet open to atmosphere. The second approach is to suck the liquid from the reservoir located well below the pump level and measure the height of water column in the tube up to which the pump drags the medium and holds it there (named “quasi priming”). It was determined that the latter two values do not necessarily exhibit the same values. Third, the most rigorous approach and the only relevant priming value is accomplished when the pump drags the water column from the reservoir below into the pumping chamber and fluid appears at the pump outlet. The height difference between a water level in a reservoir and the pump in this “real priming” gives always lower values (35–50%) than the previous two priming criteria. The differences and a noteworthy proportionality of the obtained values for a representative run of eight micropump samples are presented in **Figure 12**(left). Quality control should as well consider users scenarios such as semi dry pump priming (e.g., usage after extended periods in idle state with partially remained water inside). Micropumps have to be repeatedly tested to reveal the safety margins and to set the user specs, so the pump survives a potential misuse. In addition, self-priming is a function of actuator driving parameters, such as voltage, signal waveform, and frequency as shown in **Figure 12**(right). Here, the priming response is linear with increasing frequency for voltages below or equal 110 V, while above this

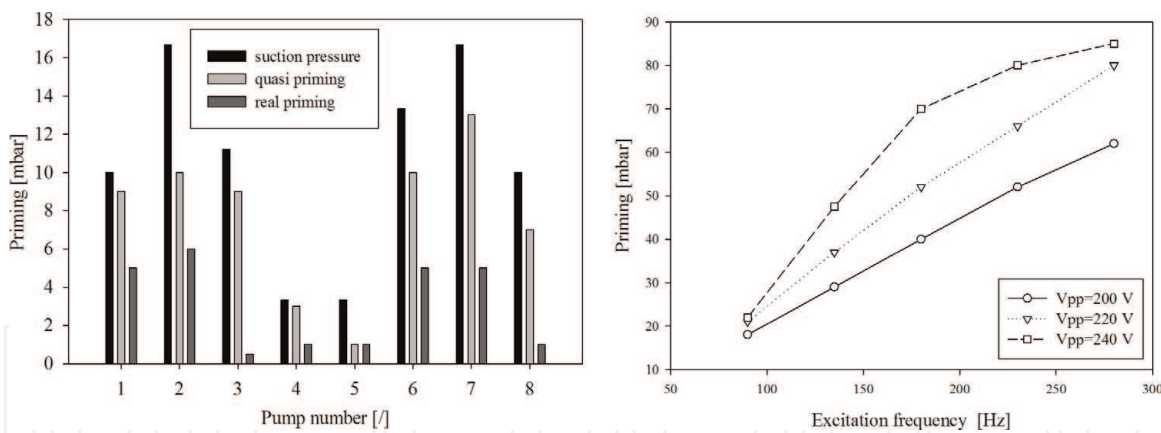


**Figure 12.** Micropump priming comparison, based on self-priming methods (left). Self-priming vs. actuator driving voltage, signal waveform and frequency (right).

value tends to be influenced by PZT degradation and/or self-heating as shown previously in **Figures 8** and **9**.

#### 5.4 Bubble tolerance

In particular cases, when the media flow in the pump supply line is disrupted by sporadic gas bubbles, formed from various reasons [14], the pump has to be able to continuously operate with both media; not only at open outlet (without load) but as well at defined load (backpressure-BP), which should be considered a common situation in real application. This is so called bubble tolerance (BT) parameter and is an additional micropump figure of merit. It is mainly a function of cylinder, throttle, and chamber design and geometry. By narrowing the gaps between membrane and cylinder/throttle and by decreasing micropump chamber depth, rectifying elements efficiency and compression ratio, respectively, are improved [15]. A combination of high rectifying elements efficiency yielding good backpressure for pumping liquid (load dependent) and high compression ratio yielding ability to pump air (expelling air from the cylinder) lead to bubble tolerant micropump. There are approaches to avoid such air bubble disruptions but require additional devices or degassing methods, which is inconvenient [14]. In our methodology, bubble tolerance test is performed by interrupting a continuous DI water flow with the introduction of air slugs, 2–4 mm long into the pump suction inlet tube (ID = 1.5 mm) every 10 seconds. This was performed as long as the water column at the outlet tube built up. Final height of output water column is proportional to the maximal backpressure at which the pump still digests air bubbles and continuous DI water pumping is ceased. The operating safe area should be set below this point, according to its known flow rate vs. backpressure characteristics. As determined empirically, qualitative criterion can be obtained as well from other measured parameters. By comparing seven measured micropump parameters for each of five pumps from the same run (**Figure 13**), it was determined that there is the strongest correlation of bubble tolerance with air flow and water backpressure performances as discussed above. In quality control process, this enables us to evaluate the property without performing explicit, time-consuming BT testing for each micropump.

#### 5.5 Temperature dependency of flow rate

It is well-known that micropump flow rate is inversely proportional to medium viscosity as given by Poiseuille expression for flow inside the microchannel. In this

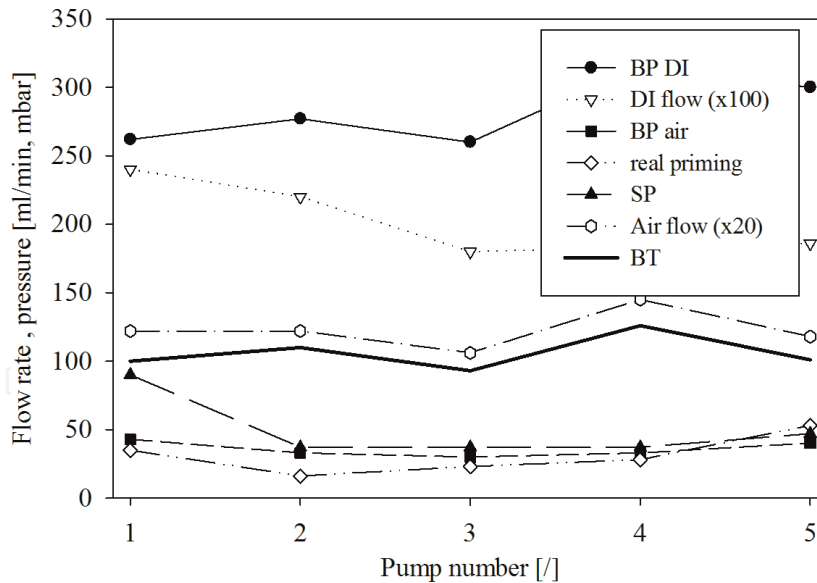


**Figure 13.**  
 Bubble tolerance correlation with other micropump performance parameters for run of five micropumps.

respect, it is further very important to take into account as well the strong temperature dependency of the medium viscosity, which is additionally affecting the flow-pressure performance. For example, water dynamic viscosity is known from the literature to decrease by ca. 30% in the temperature range between 20 and 35°C, while the water density decreases only by 0.4% in the same temperature range and is therefore negligible if we want to introduce correction method. It was experimentally determined that for deionized water, the increase of flow rate with temperature closely follows the well-known decrease of viscosity but only up to 42°C (**Figure 14**). As shown, flow rate above this temperature tends to decrease rapidly. It is assumed that above this point, the temperature dependency of material properties, such as PDMS and PZT actuator tend to deteriorate the pump performances. Besides, at higher temperature, additional microfluidic phenomena such as degassing and cavitation might contribute to flow rate decrease. Based on these experimental data, we included the above temperature-dependent viscosity

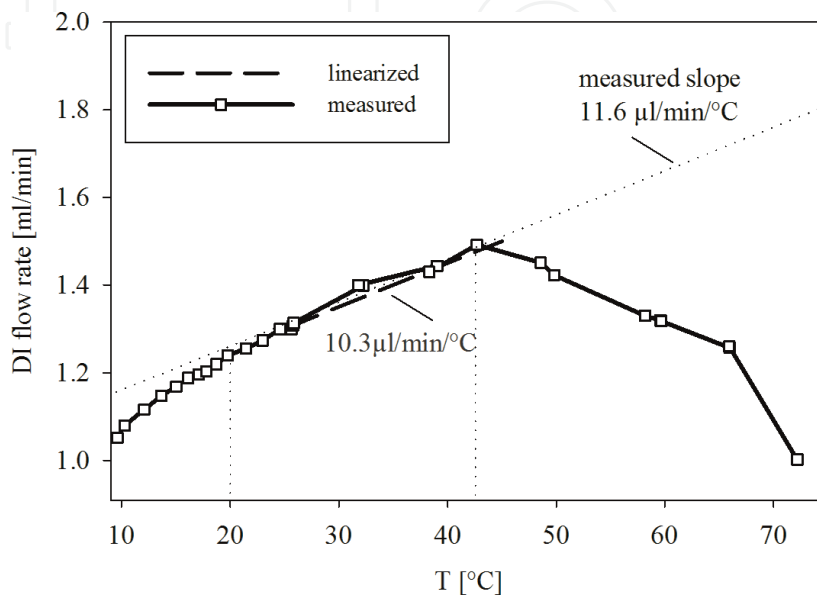


**Figure 14.**  
 Pump flow rate vs. DI water temperature.

correction factor in the results of our long-term flow rate stability tests as shown in **Figure 15**. Two micropumps were continuously pumping DI water in closed loop for a period of 27 weeks without particular ambient temperature control. The temperature and flow rate variations were measured periodically. It is very evident that flow rate variations (lines without symbols) are closely related to temperature variations (**Figure 14**, full circles). By implementing the correction for a temperature dependency of viscosity obtained from **Figure 15**, the apparent flow rate variations were mitigated, meaning that pump performed more stable than shown by raw data. In general, taking into account the correction around reference temperature, 20°C, which accounted for 0.9%/°C the flow rate variations for pump A is realistically improved from a 26% decrease over 27 weeks to 12% and similarly for pump B (**Figure 15**, hollow symbols).

## 5.6 Heat dissipation

In most applications, PZT actuators are driven at high electric field magnitudes and/or high frequencies. Beside the useful conversion into mechanical work, a significant amount of heat is generated within nonideal PZT. Heat generation can considerably affect the reliability and piezoelectric properties of micropump actuators, and may also limit their application since it heats the adjacent materials, and at last but not least also the pumping medium. Self-heating, that is, heat generation within the piezoelectric actuator due to electrical and mechanical losses, is a major concern for high-frequency applications, where increased stress and even degradation of the actuator is expected. In sinusoidal excitation, the average power dissipation  $P$  in a piezoelectric actuator can be estimated using the expression below,

$$P = \frac{\pi}{4} f C \tan \delta U_{pp} \quad (1)$$

where  $\tan \delta$  is the dielectric dissipation factor,  $C$  is apparent PZT actuator capacitance,  $U_{pp}$  is peak-to-peak operating voltage, and  $f$  is the operating frequency.

To be able to evaluate the thermal response of the micropump as a thermal system, it is necessary to know the geometry and thermal properties of individual materials such as thermal conduction, free surfaces, fluid type, and flow for the

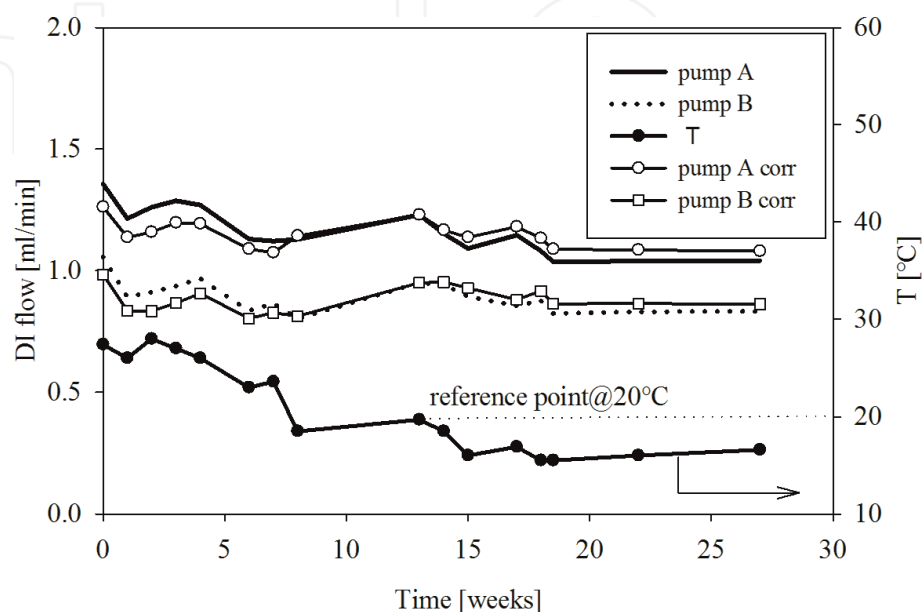


**Figure 15.** Long-term testing and flow rate correction due to temperature dependent viscosity of water.

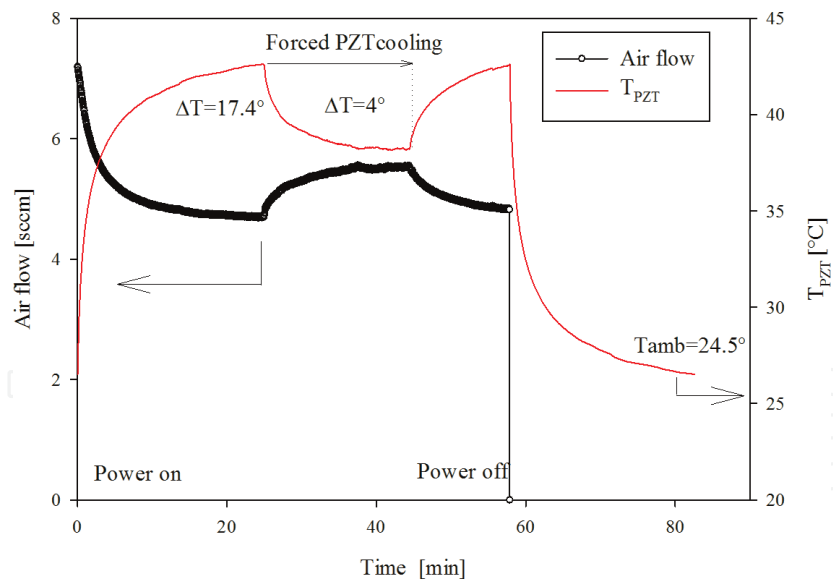


**Figure 16.**  
*Interrelation of temperature due to PZT heat dissipation and micropump air flow rate.*

evaluation of natural or forced convection. It has to be noted as well that piezo ceramics has low heat conductivity but rather high heat capacity, which affects the thermal time constants. It can be found in the literature that for a standard PZT actuator under small-signal conditions, up to 2% of the electrical energy flowing through the actuator is converted into heat. In large-signal conditions, however, 8–12% of the electrical energy pumped into the actuator is converted to heat. Therefore, increased operating temperature can strongly affect the piezo actuator dynamics.

Our recommended approach to determine and characterize how a particular micropump system behaves thermally is to monitor temperature of PZT and/or pumping medium directly by using a temperature sensor mounted on/near the PZT and perform measurements during the micropump operation. This should be correlated with measurements of flow rate or other performance variations. A miniature Pt-100 temperature sensor in our case was mounted atop the PZT disc with special emphasis not to disturb the operation and minimize damping. Once knowing the temperature conditions of PZT, temperature sensor can be placed next to PZT on glass membrane for continuous monitoring purposes.

A very illustrative example of interrelation between PZT temperature and air flow rate is given in **Figure 16** for micropump driven at normal actuating regime. The proposed type of measurements is very useful particularly in pumping systems, where high-flow rate accuracy is required. The measured temperature dependency of flow rate can be further included in compensation algorithm of control loop.

## 6. Conclusion

For a case study of piezoelectric micropumps quality control, an innovative microcylinder pump developed in our laboratory was selected. Quality control is given by extensive evaluation methodology for assessing mechanical properties of constituent micropump components (Young's modulus of PDMS elastomer and  $d_{31}$  modulus of PZT actuator), reliability, and stability of micropump operation (self-priming, bubble tolerance, pumping media chemical compatibility, and heat dissipation) and quality of fabrication process (covalent bond strength, bond hydrolytic stability, and plastic housing surface flatness). Namely, irregular flatness of ABS

substrate directly transfers on the membrane via PDMS elastomer layer. This results in sticking of rectifying elements thus causing micropump malfunction. It is shown herein that micropump operating stability is closely related to PZT excitation signal amplitude, which might cause deterioration of piezoelectric actuator. Degradation of  $d_{31}$  modulus due to PZT depolarization or fatigue directly effects micropump flowrate and backpressure performance. In this respect, safe operating area needs to be determined. The methodology to determine self-priming ability criteria is given. It is further shown that in quality control of micropump operation, the bubble tolerance can be estimated indirectly through the micropump airflow and water backpressure performance. Finally, it is shown that temperature dependency of flow rate has to be taken into account. It was determined that it reflects mainly through variations in viscosity at lower temperatures and temperature dependency of material properties of PZT and PDMS at elevated temperature.

## Acknowledgements

This work was performed within the framework of a project supported by the Slovenian industrial partner KOLEKTOR Group d.o.o., Vojkova 10, 5280 Idrija Slovenia and the Ministry of Education, Science, Culture and Sport (Grant No P2-0244).

IntechOpen

## Author details

Matej Možek\*, Borut Pečar, Drago Resnik and Danilo Vrtačnik  
Laboratory of Microsensor Structures and Electronics (LMSE), Faculty of Electrical Engineering, University of Ljubljana, Ljubljana, Slovenia

\*Address all correspondence to: [matej.mozek@fe.uni-lj.si](mailto:matej.mozek@fe.uni-lj.si)

## IntechOpen

© 2019 The Author(s). Licensee IntechOpen. This chapter is distributed under the terms of the Creative Commons Attribution License (<http://creativecommons.org/licenses/by/3.0>), which permits unrestricted use, distribution, and reproduction in any medium, provided the original work is properly cited. 

## References

- [1] Kamei KI, Kato Y, Hirai Y, Ito S, Satoh J, Oka A, et al. Integrated heart/cancer on a chip to reproduce the side effects of anti-cancer drugs in vitro. *RSC Advances*. 2017;7(58):36777-36786
- [2] Minter S. *Alcoholic Fuels*. CRC Press; 2016
- [3] Liu Y, Li G. A power-free, parallel loading microfluidic reactor array for biochemical screening. *Scientific Reports, Nature*. 2018;8(1):13664
- [4] Vijaya MS. *Piezoelectric Materials and Devices: Applications in Engineering and Medical Sciences*. CRC Press; 2016
- [5] Dolžan T, Pečar B, Možek M, Resnik D, Vrtačnik D. Self-priming bubble tolerant microcylinder pump. *Sensors and Actuators A: Physical*. 2015;233:548-556
- [6] Suzuki Y, Yamada M, Seki M. Sol-gel based fabrication of hybrid microfluidic devices composed of PDMS and thermoplastic substrates. *Sensors and Actuators B: Chemical*. 2010;148(1):323-329
- [7] Tsao CW, DeVoe DL. Bonding of thermoplastic polymer microfluidics. *Microfluidics and Nanofluidics*. 2009;6(1):1-16
- [8] Wu J, Lee NY. One-step surface modification for irreversible bonding of various plastics with a poly (dimethylsiloxane) elastomer at room temperature. *Lab on a Chip*. 2014;14(9):1564-1571
- [9] Pečar B, Možek M, Vrtačnik D. Thermoplastic-PDMS polymer covalent bonding for microfluidic applications. *Informacije MIDEM*. 2017;47(3):147-154
- [10] Lee SK, Lee H, Ram JR. U.S. Patent No. 9,422,409. Washington, DC: U.S. Patent and Trademark Office; 2016
- [11] Lee KS, Ram RJ. Plastic-PDMS bonding for high pressure hydrolytically stable active microfluidics. *Lab on a Chip*. 2009;9(11):1618-1624
- [12] Johnston ID, McCluskey DK, Tan CKL, Tracey MC. Mechanical characterization of bulk Sylgard 184 for microfluidics and microengineering. *Journal of Micromechanics and Microengineering*. 2014;24(3):035017
- [13] Genenko YA, Glaum J, Hoffmann MJ, Albe K. Mechanisms of aging and fatigue in ferroelectrics. *Materials Science and Engineering: B*. 2015;192:52-82
- [14] Jenke C, Kager S, Richter M, Kutter C. Flow rate influencing effects of micropumps. *Sensors and Actuators A: Physical*. 2018;276:335-345
- [15] Richter M, Linnemann R, Woias P. Robust design of gas and liquid micropumps. *Sensors and Actuators*. 1998